ADVANCED MATERIALS
www.advmat.de

www.MaterialsViews.com

A Thieno[3,2-*b*][1]benzothiophene Isoindigo Building Block for Additive- and Annealing-Free High-Performance Polymer Solar Cells

Wan Yue, Raja Shahid Ashraf, Christian B. Nielsen, Elisa Collado-Fregoso, Muhammad R. Niazi, Syeda Amber Yousaf, Mindaugas Kirkus, Hung-Yang Chen, Aram Amassian, James R. Durrant, and Iain McCulloch*

Organic photovoltaics (OPV) have attracted considerable attention over the last two decades as an emerging candidate to contribute toward renewable energy due to features such as mechanical flexibility, light weight, and the capability to fabricate large area devices via room temperature solution processing techniques.[1] Encouragingly, power conversion efficiencies (PCEs) of over 10% have already been realized in single-junction bulk-heterojunction (BHJ) polymer solar cells (PSC) based on interpenetrating fullerene acceptors and conjugated polymer donor domains.[2] However, this recent progress has been mainly achieved with the utilization of additives, charge extraction layers, and post-solvent/thermal annealing procedures.[3–5] Considering manufacturing challenges for future commercialization of solar cells, high-performance active layer materials based on new building blocks are still required which can enable a simplified device architecture, fabricated without additives, or thermal annealing and no additional interlayer for realizing high-throughput, low-cost products.[6–8]

Conjugated polymers containing alternating electron-rich and electron-deficient repeat units have emerged as a popular concept in the design of low band gap active layer materials. Fused aromatic/heteroaromatic subunits, creating ladder-type polymers, provide enforced rigidity and coplanarity, which reduces rotational disorder thus lowering molecular reorganization energy and facilitates charge transport.[9,10] Some of the highest performing polymers for organic semiconductors utilize this concept.[11,12] Of these high performing materials, isoindigo is one of the most versatile structural motifs.

Isoindigo comprises an electron-deficient symmetrical lactam core fused with aromatic groups, initially phenyl. It possesses an off-axis dipole moment, facilitated by the carbonyl functionality, which promotes strong intermolecular interactions. Solubility and bulk morphology can be optimized by the incorporation of alkyl chains on the lactam nitrogen positions, with both energy level and polymer conformation tuning possible through the choice of aromatic flanking groups and co-repeat units. Significant progress in isoindigo containing polymers has resulted in high PCEs for solar cells and high charge-carrier mobility for organic thin film transistors (OTFTs).[13–15] However, there have been only a few attempts to modify the basic isoindigo skeleton. Alternative aromatic groups to phenyl have been recently reported, including both thiophene flanked isoindigo and thieno[3,2-*b*]thiophene isoindigo copolymers, both of which were reported to have high charge transport and ambipolar characteristics in thin film OFET devices.[16,17] The thiophene flanking unit, in comparison to phenyl, can reduce the dihedral angle between linking repeat units, enhancing both intramolecular pi electron conjugation as well as facilitating pi–pi stacking and consequently improved charge transport. Additionally, extending the size of the unit, through an additional fused thiophene, has been shown to reduce the polymer conformational and energetic disorder, improving polaron delocalization and charge transport. However, high-efficiency OPV devices with these polymers as electron donors were not achieved, attributed to their relatively high highest occupied molecular orbital (HOMO) levels arising from the electron-rich thiophene heterocycle groups. Consequently, the molecular design approach of this work was targeted to simultaneously reduce the electron density of the thiophene isoindigo polymers, while retaining the large fused conjugated structure which incorporates thiophene flanking units. This has been achieved by incorporating two thieno[3,2-*b*][1]benzothiophene (TBT) units flanking the isoindigo core. Utilization of the TBT simultaneously significantly extends the effective fused planar aromatic area, improving pi-orbital overlap and increases coplanarity along the backbone.[18] Copolymers based on this novel eight-ring thieno[3,2-*b*][1]benzothiophene isoindigo (TBTI) acceptor unit were synthesized and their performance in BHJ devices reported.

Dr. W. Yue, Dr. R. S. Ashraf, Dr. C. B. Nielsen, E. Collado-Fregoso, Dr. M. Kirkus, Dr. H.-Y. Chen, Prof. J. R. Durrant, Prof. I. McCulloch
Department of Chemistry
and Centre for Plastic Electronics
Imperial College London
London SW7 2AZ, UK
E-mail: w.yue@imperial.ac.uk

M. R. Niazi, Prof. A. Amassian, Prof. I. McCulloch
Physical Sciences and Engineering Division
King Abdullah University of Science and Technology (KAUST)
Thuwal 23955-6900, Saudi Arabia

S. A. Yousaf
Department of Physics
Government College University
Lahore 54000, Pakistan

DOI: 10.1002/adma.201501841

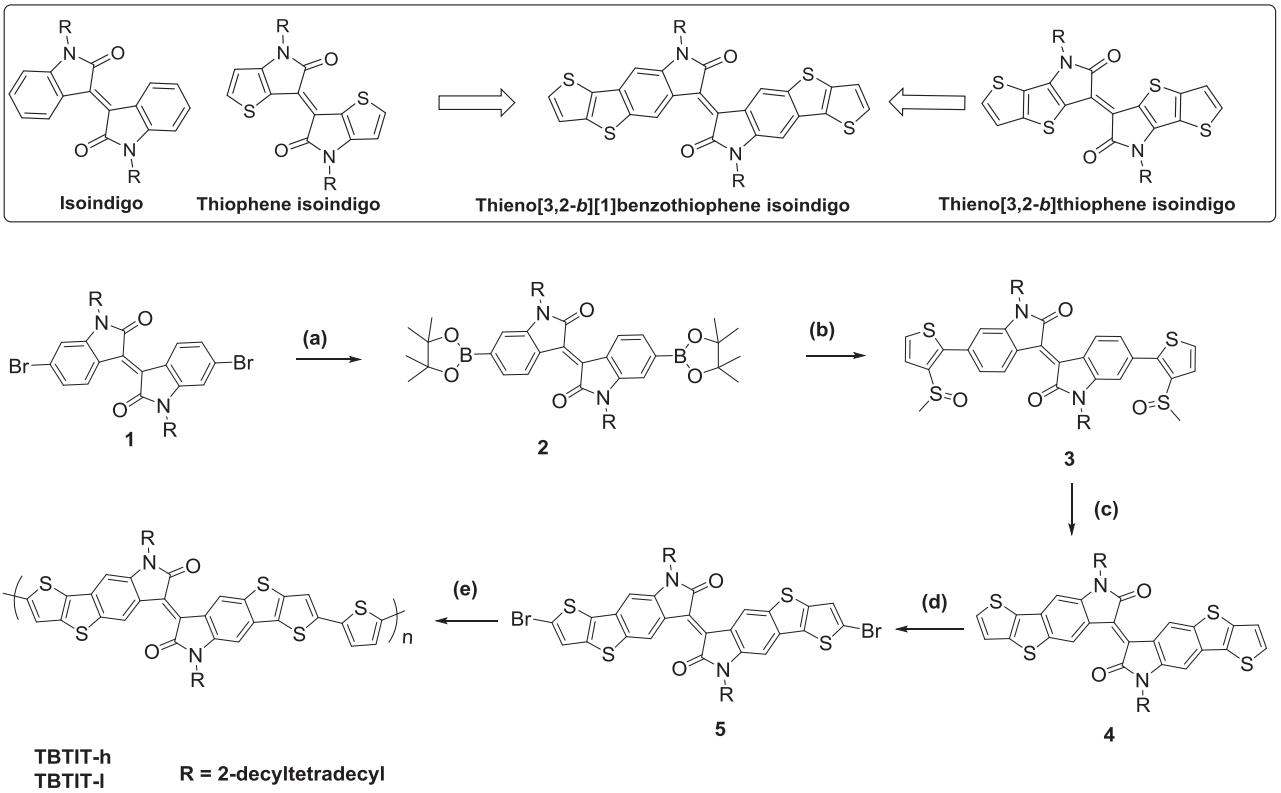

Figure 1. Structures of isoindigo derivatives and synthesis route of monomer and polymer. a) Bis(pinacolato)diboron, $Pd(PPh_3)_2Cl_2$, AcOK, anhydrous toluene, reflux, 16 h; b) bromo-3-methylsulfinylthiophene, $Pd_2(dba)_3$, P(*o*-tol)$_3$, aq. K_3PO_4, toluene, reflux, 18 h; c) Eaton's reagent, rt, 3d, then pyridine, reflux, overnight; d) NBS, $CHCl_3$/AcOH, reflux, 5h; e) bis(trimethylstannyl)thiophene, $Pd_2(dba)_3$, P(*o*-tol)$_3$, chlorobenzene, μW.

The molecular weight of conjugated polymers is a key factor in determining their optical-electrical, morphological, and performance properties.[19] For low band gap polymer/fullerene systems utilized in OPV, high molecular weight polymers generally induce improved charge transport and device performance over their lower molecular weight counterparts.[20] However, solubility issues can arise when the molecular weight is high, presenting problems in processing. In this study, two significantly different number-average molecular weights (M_n) of 151 and 33 kDa were synthesized and the effect of molecular weight on the optical-electrical, morphological, photovoltaic, and processing performance was investigated.

The synthetic procedure for TBTIT is depicted in **Figure 1**. 6,6′-dibromoisoindigo (**1**) was synthesized according to the literature.[21] The branched 2-decyltetradecyl chain was attached at the amide position to ensure sufficient solubility of the resulting polymer. Pd-catalyzed Miyaura borylation between **1** and bis(pinacolato)diboron furnished **2** in a good yield,[22] which was then reacted with bromo-3-methylsulfinylthiophene under typical Suzuki reaction conditions, providing desired intermediate **3**. The critical last step was performed with Eaton's reagent followed by demethylation[23] to afford the novel π-extended building block TBTI in a moderate yield. TBTI was subsequently brominated with *N*-bromosuccinimide (NBS) to give the final monomer **5**. Finally, polymers TBTIT-h and TBTIT-l were obtained by copolymerizing **5** with bis-stannylated thiophene, using palladium-catalyzed microwave Stille coupling reaction in chlorobenzene. By controlled variation of the polymerization temperature and time, it was possible to synthesize two different molecular weights, with very high molecular weight possible due to optimal choice of catalyst, conditions, and stoichiometric control of high purity monomers. Full synthetic details and characterization of the monomer and polymers are described in the Supporting Information. The higher molecular weight batch exhibited an M_n of 151 kDa with a polydispersity index (PDI) of 3.6, with lower molecular weight batch having an M_n of 33 kDa with a PDI of 2.7 (**Table 1**), as determined

Table 1. Molecular weight, optical properties, and energy levels of polymers TBTIT-h and TBTIT-l.

Polymer	M_n[a)] [kDa]	M_w[a)] [kDa]	PDI[a)]	$\lambda_{max(film)}$ [nm]	IP[b)] [eV]	EA[c)] [eV]	E_g[d)] [eV]	E_{HOMO}[e)] [eV]	E_{LUMO}[e)] [eV]
TBTIT-h	151	546	3.6	665	5.1	3.5	1.6	−5.0	−3.0
TBTIT-l	33	91	2.7	660	5.2	3.6	1.6	−5.0	−3.0

[a)] M_n, M_w, and PDI (M_w/M_n) determined by GPC using low-D (<1.10) polystyrene standards and chlorobenzene as the eluent at 80 °C; [b)] Estimated using PESA; [c)] Estimated by adding E_g to IP; [d)] Estimated from the onset of UV–vis absorption spectrum; [e)] Calculated using TD/DFT calculations with B3LYP/6-311G(d).

by size-exclusion chromatography (SEC) relative to monodisperse polystyrene standards. Both polymer batches are soluble in chlorobenzene (CB) and *o*-dichlorobenzene (DCB). Thermogravimetric analysis (TGA) demonstrated that the polymers were thermally stable up to a decomposition temperature with a 5% weight loss at 420 °C for TBTIT-h and 405 °C for TBTIT-l respectively (Figure S1, Supporting Information). No discernible thermal transitions were observed for either polymer molecular weights when analyzed by differential scanning calorimetry (DSC) in the temperature range of 0–300 °C (Figure S2, Supporting Information).

In contrast to isoindigo, which exhibits a maximum absorption at 500 nm with a molar extinction coefficient (ε) of 3940 M^{-1} cm^{-1} in the visible region,[24] the TBTI unit shows a slightly redshift absorption with an absorption peak at 510 nm with almost an order of magnitude higher ε of 36 700 M^{-1} cm^{-1} (Figure S3, Supporting Information). We note that the increased molecular orbital overlap between the HOMO and lowest unoccupied molecular orbital (LUMO) of the aromatic system, originating from a more extended effective conjugated length of TBTI, can contribute to enhance the molar extinction coefficient of the monomer.[25] Both the polymer molecular weights display similar absorption spectra in solution and thin films (**Figure 2**a and Figure S4, Supporting Information), with an absorption maximum at 665 nm for TBTIT-h and 660 nm for TBTIT-l. The molar extinction coefficients were found to be 6.2×10^4 M^{-1} cm^{-1} for both polymers in solution, higher than that of the analogous isoindigo thiophene copolymer (5.3×10^4 M^{-1} cm^{-1}),[26] while absorption coefficients of 6.9×10^4 cm^{-1} for TBTIT-h and a slightly lower value of 6.5×10^4 cm^{-1} for TBTIT-l were found in the solid state. This slightly redshifted absorption spectra and more pronounced long wavelength shoulder for the higher molecular weight polymer is indicative of enhanced aggregation. Indeed, temperature-dependent solution UV studies show both a blueshift and disappearance of the long wavelength shoulder at increasing temperature (Figure S5, Supporting Information). The long wavelength absorption peak is typical of intramolecular charge-transfer character from the thiophene unit to the TBTI core, and its high intensity, confirming the strong electron withdrawing property of the TBTI unit. This is also in accordance with the computational results that show the HOMO is delocalized along the polymer chain, while the LUMO is mostly localized on the TBTI core (Figure 2b). Because of the steric encumbrance effect involving the outer sulfur atoms of the TBTI and the neighboring sulfur atom of the thiophene ring, the B3LYP/6-31G*-optimized geometries of TBTIT trimer predict the "anti" sulfur arrangement with a relatively planar structure corresponding to the lowest energy (Figure 2b). Both polymers show similar electronic energy levels with an IP of 5.1 eV for TBTIT-h and 5.2 eV for TBTIT-l, estimated by photoelectron spectroscopy in air (PESA) (Table 1). In the solid state, both molecular weights exhibit an optical band gap (E_g) of 1.6 eV, as

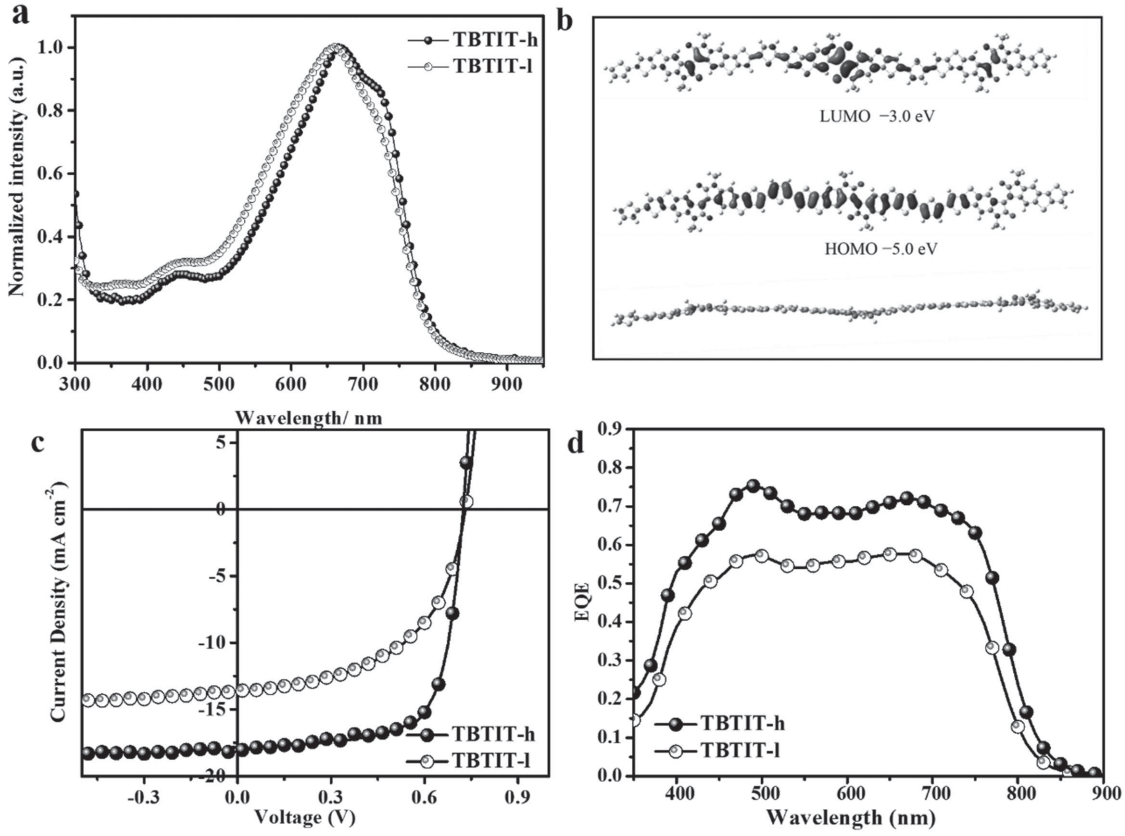

Figure 2. a) Normalized UV–vis absorption spectra of TBTIT-h and TBTIT-l in solid thin film on quartz; b) DFT-calculated HOMO and LUMO wave functions of the geometry optimized structures (B3LYP/6-31G) of the TBTI-T trimer model of the studied polymers with the minimum energy conformation; c) the *J*–*V* curves of PSCs based on polymer: $PC_{71}BM$ (1:2 w/w); d) EQE curves of the corresponding devices.

Table 2. Charge transport and OPV device performance characteristics of polymers TBTIT-h, and TBTIT-l with $PC_{71}BM$ fullerene acceptors (polymer:fullerene 1:2 w/w blend ratio) using an inverted device architecture.

Polymer	μ_h (TFT) [$cm^2\ V^{-1}\ s^{-1}$]	J_{sc} [a)] [$mA\ cm^2$]	V_{oc} [V]	FF	PCE [b)] [%]
TBTIT-h	0.31	17.7	0.72	0.71	9.1
TBTIT-l	0.15	13.6	0.73	0.54	5.3

[a)] EQE corrected; [b)]ITO/ZnO/active layer (polymer: $PC_{71}BM$ (w/w))/MoO_3/Ag), treatment of ZnO layer with 1% ethanol amine (EA) in 2-methoxyethanol.

determined by the onset of the absorption spectrum (785 and 795 nm). We note that an IP around 5.2 eV and a band gap of roughly 1.5 eV have been modeled to be optimal for a single cell OPV due to a sufficient energetic driving force for electron transfer and an optimal spectral overlap with the solar flux.[27]

To investigate and compare the photovoltaic properties of both molecular weight polymers, polymer/fullerene bulk heterojunction solar cells in an inverted device architecture[28,29] were fabricated with $PC_{71}BM$ as the acceptor material. The active layers were spun cast from DCB solution at room temperature. Polymer (TBTIT-h):fullerene weight ratios of 1:1.5, 1:2, 1:2.5, and 1:3 were evaluated (Table S1 and Figure S6, Supporting Information), and it was found that a 1:2 weight ratio of polymer to fullerene was optimal. The photovoltaic characteristics of the devices under simulated AM 1.5 G irradiation with intensity of 100 mW cm^{-2}, including the corresponding J_{sc}, FF, and V_{oc} are summarized in **Table 2**. Figure 2c shows the current–voltage (J–V) curves of the best device. A similar V_{oc} of 0.72 V was observed for high molecular weight polymer and 0.73 V for low molecular weight polymer. Differences in J_{sc} and FF values between the molecular weights were evident however. A high J_{sc} of 17.7 mA cm^2 and a high FF of 0.71 were observed for TBTIT-h. TBTIT-l, however, exhibited a lower J_{sc} of 13.6 mA cm^2 and an FF of 0.54. A PCE of 9.1% was observed for TBTIT-h, while the lower molecular weight TBTIT-l exhibited a lower PCE of 5.3%. This is the highest PCE reported in a standard conventional or inverted device configuration without using any additive or postsolvent/thermal annealing during the fabrication process, and is also the highest OPV efficiency reported so far for isoindigo polymers. The external quantum efficiency (EQE) curves for the best devices are shown in Figure 2d. A broad spectral response in the 400–800 nm region with relatively flat EQE profiles was observed for both devices, with the maximum observed around 490 nm where both the polymers and $PC_{71}BM$ absorb, with peak EQE values of about 76% for TBTIT-h and 58% for TBTIT-l. The high efficiency extends to over 700 nm, predominantly due to the polymer long wavelength absorption.

The difference in polymer molecular weight influences thin film crystallinity, resulting in different phase morphology of the BHJ blends, thereby influencing the charge separation and charge carrier mobility.[30] From XRD diffractograms of thick drop-cast films of neat polymers (Figure 4a), we observe clear diffraction peaks from the periodic lamellar spacing but no peaks from pi-pi stacking, which indicates that both polymers orient predominantly edge-on relative to the substrate. The lamellar distance is 20.5 Å for TBTIT-h with a strong peak intensity. In contrast, TBTIT-l exhibits only a relatively weak diffraction peak corresponding to a lamellar distance of 20.9 Å. The higher degree of crystallinity of TBTI-T-h is also evident from a more significant second order peak (200) and a visible third order peak (300). Upon thermal annealing, lamellar distances change slightly to 20.9 Å for TBTIT-h and 21.1 Å for TBTIT-l. The higher degree of crystallinity of TBTI-T-h is also evident from a more significant second-order peak (200) and a visible third-order peak (300), and the peak of (200) furthermore increases in intensity upon thermal annealing at 100 °C. Thermal annealing is seen to reduce the diffractogram peak widths for both polymers, indicating the formation of larger crystallites upon annealing. Atomic force microscopy (AFM) and energy-filtrated transmission electron microscopy (EFTEM) were used to further investigate the microstructure and surface morphologies of both blends (**Figure 3**). EFTEM images reveal that both blends exhibit optimal, phase-separated, bicontinuous interpenetrating networks with average domain sizes of about 10 nm. AFM measurements show that the TBTIT-l:$PC_{71}BM$ blend exhibits a root-mean-square (RMS) roughness of 1.29 nm and a phase-separated morphology with apparently slightly larger aggregates of polymer and $PC_{71}BM$. In contrast, the TBTIT-h:PC71BM blend shows a smoother and more defined nanoscale morphology with a finely intermixed and homogenous phase separation and slightly lower RMS roughness of 0.83 nm.

Thin film transistor devices (TFT) were used to investigate the polymer hole transport. The polymers exhibit promising p-type transistor performance, superior to the analogous isoindigo thiophene copolymer,[31] with saturated charge carrier mobilities up to 0.31 $cm^2\ V^{-1}\ S^{-1}$ for TBTIT-h and 0.15 $cm^2\ V^{-1}\ S^{-1}$ for TBTIT-l thin films after thermal annealing at 150 °C (**Figure 4**b,c and Figure S7, Supporting Information). The larger mobility of the higher molecular weight polymer correlates well with the observed increase in crystallinity observed by XRD diffractograms (Figure 4a). This larger hole mobility of the TBTIT-h, and a more optimal nanoscale morphology, contribute to the improvement in OPV performance of TBTIT-h, particularly the increase in J_{sc} and FF. This result highlights the importance of achieving high molecular weight for both OPV and FET performance.

Photoluminescence quenching (PLQ) experiments were carried out on polymer: $PC_{71}BM$ blend films as well as neat films, as shown in Figure S8 (Supporting Information). Both molecular weight blends were observed to have a relatively high polymer PLQ (slightly below 90%) with some polymer emission remaining. In contrast to very amorphous polymers, in which the polymer PL is usually at least 98% quenched,[32] this lower extent of quenching is consistent with a higher degree of polymer crystallinity, with a concomitant $PC_{71}BM$ expulsion. It is possible to estimate the size of these relatively polymer pure domains to be around 3.3 nm,[32] which is appropriate for good exciton dissociation.[33] It is important to remark, however, that the polymer PLQ values are very similar for both molecular weights; therefore, the differences in the EQE that correspond to the polymer contribution are not due to difference in exciton quenching. Furthermore, there is a remaining ≈20% of $PC_{71}BM$ PL in both cases, which suggests the existence of relatively pure fullerene domains, similar to what has been observed for other high-performing systems.[34,35] The presence

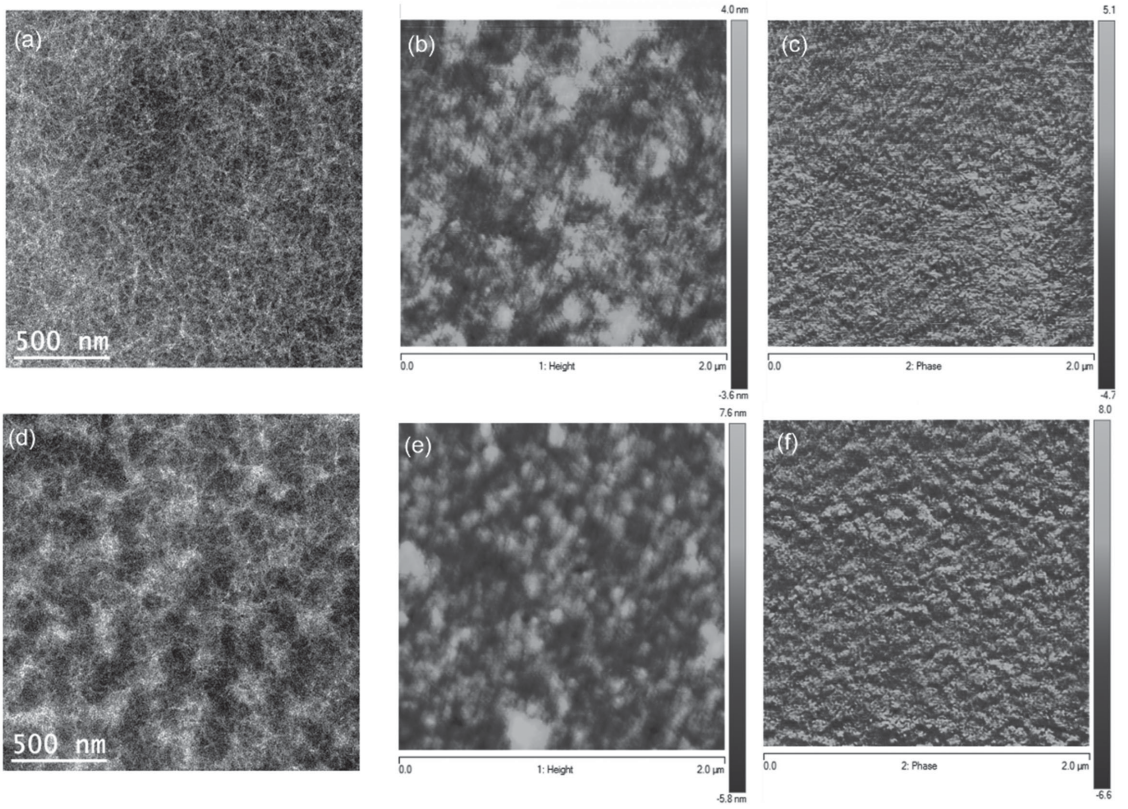

Figure 3. Energy-filtered TEM and tapping-mode AFM topography, and phase images of blend films based on polymer TBTIT-h/$PC_{71}BM$ (1:2, w/w) (a–c) and TBTIT-l/$PC_{71}BM$ (1:2, w/w) (d–f) cast from DCB. The sizes of the AFM images are 2 µm × 2 µm.

of relatively extended $PC_{71}BM$ pure, crystalline regions has been correlated with an additional driving energy to separate polaron pairs as well as induce a better percolation pathway for an improved charge transport. In general, for both molecular weights we observe a relatively good polymer and $PC_{71}BM$ exciton quenching which is reflected in the rather flat EQE profiles of the respective devices.

In conclusion, a novel versatile eight-ring fused isoindigo-based acceptor TBTI incorporating two thieno[3,2-*b*][1]benzothiophene units was synthesized efficiently. Copolymerization with thiophene afforded two different molecular weight (TBTIT-h and TBTIT-l) polymers with high absorption coefficients and optimal band gaps for organic photovoltaics application. The single junction PSC devices derived from TBTIT-h:$PC_{71}BM$ blends exhibit efficiencies up to 9.1% with a high J_{sc} of 17.7 mA cm^2 and a high FF of 0.71 for as-cast films without using any additives or postsolvent/thermal annealing steps during the device fabrication. The superior PCE of the TBTIT-h was shown to originate from higher degree of crystallinity, more optimal blend morphology, and higher charge carrier mobility.

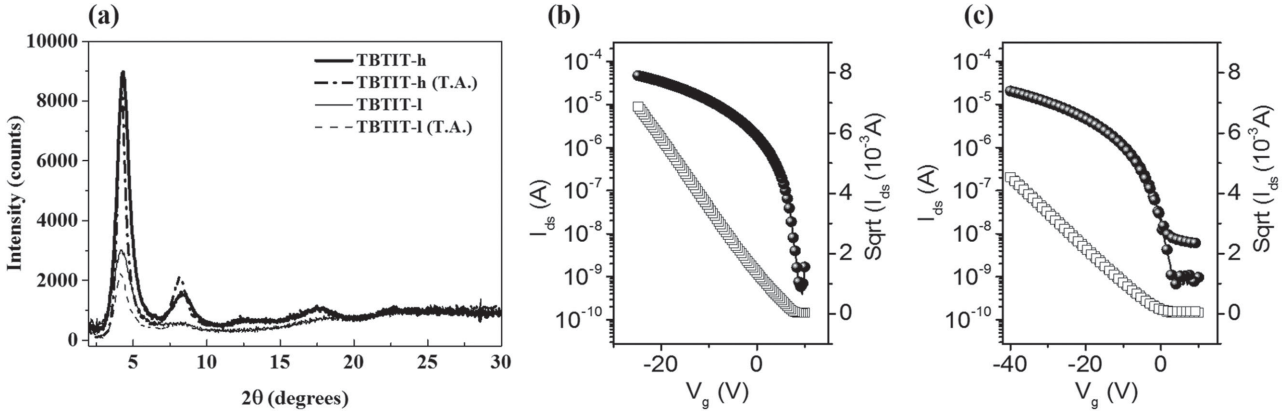

Figure 4. a) XRD diffractograms of thick drop cast films (from 5 mg mL^{-1} chlorobenzene solution) of TBTIT-h (thick solid line) and TBTIT-l (thin solid line) measured and after annealing for TBTIT-h (dot-dashed line) and TBTIT-l (dashed line) at 100 °C for 20 min in an inert atmosphere; b,c) transfer characteristics of polymer TBTIT-h (b) and TBTIT-l (c) after thermal annealing at 150 °C.

These results demonstrate that TBTI could be a highly promising building block for high-efficiency polymer OPV devices.

Supporting Information

Supporting Information is available from the Wiley Online Library or from the author.

Acknowledgements

This work was supported by Marie Curie Intra-European Fellowship with the 7th European Community Framework Programme (FP7-PEOPLE-2013-IEF-622187). The authors thank Dr. Fiona Scholes for AC-2 PESA measurement and EC FP7 Project SC2, EC FP7 Project ArtESun, EC FP7 Project PolyMed, and EPSRC Project EP/G037515/1 for financial support.

Received: April 17, 2015
Revised: May 16, 2015
Published online: July 14, 2015

[1] Y. J. Cheng, S. H. Yang, C. S. Hsu, *Chem. Rev.* **2009**, *109*, 5868.
[2] M. C. Scharber, N. S. Sariciftci, *Prog. Polym. Sci.* **2013**, *38*, 1929.
[3] Z. He, B. Xiao, F. Liu, H. Wu, Y. Yang, S. Xiao, C. Wang, T. P. Russell, Y. Cao, *Nat. Photonics* **2015**, *9*, 174.
[4] C. Cabanetos, A. ElLabban, J. A. Bartelt, J. D. Douglas, W. R. Mateker, J. M. J. Frechet, M. D. McGehee, P. M. Beaujuge, *J. Am. Chem. Soc.* **2013**, *135*, 4656.
[5] X. Guo, N. Zhou, S. J. Lou1, J. Smith, D. B. Tice1, J. W. Hennek, R. P. Ortiz, J. T. L. Navarrete, S. Li, J. Strzalka, L. X. Chen, R. P. H. Chang, A. Facchetti, T. J. Marks, *Nat. Photonics* **2013**, *7*, 825.
[6] C. B. Nielsen, R. S. Ashraf, N. D. Treat, B. C. Schroeder, J. E. Donaghey, A. J. P. White, N. Stingelin, I. McCulloch, *Adv. Mater.* **2015**, *27*, 948.
[7] J. Woong, F. Liu, T. P. Russell, W. H. Jo, *Adv. Energy Mater.* **2015**, DOI: 10.1002/aenm.201500065.
[8] W.-H. Chang, L. Meng, L. Dou, J. You, C-C. Chen, Y. Yang, E. P. Young, G. Li, Y. Yang, *Macromolecules* **2015**, *48*, 562.
[9] I. McCulloch, R. S. Ashraf, L. Biniek, H. Bronstein, C. Combe, J. E. Donaghey, D. I. James, C. B. Nielsen, B. C. Schroeder, W. Zhang, *Acc. Chem. Res.* **2012**, *45*, 714.
[10] J-S. Wu, S-W Cheng, Y-J. Cheng, C-S. Hsu, *Chem. Soc. Rev.* **2015**, *44*, 1113.
[11] Y-X. Xu, C.-C. Chueh, H.-L. Yip, F.-Z. Ding, Y.-X. Li, C.-Z. Li, X. Li, W.-C. Chen, A. K.-Y. Jen, *Adv. Mater.* **2012**, *24*, 6356.
[12] Y. Wu, Z. Li, W. Ma, Y. Huang, L. Huo, X. Guo, M. Zhang, H. Ade, J. Hou, *Adv. Mater.* **2013**, *25*, 3449 .
[13] E. Wang, W. Mammo, M. R. Andersson, *Adv. Mater.* **2014**, *26*, 1801.
[14] T. Lei, J.-Y. Wang, J. Pei, *Acc. Chem. Res.* **2014**, *47*, 1117.
[15] Y. Deng, J. Liu, J. Wang, L. Liu, W. Li, H. Tian, X. Zhang, Z. Xie, Y. Geng, F. Wang, *Adv. Mater.* **2014**, *26*, 471.
[16] I. Meager, M. Nikolka, B. C. Schroeder, C. B. Nielsen, M. Planells, H. Bronstein, J. W. Rumer, D. I. James, R. S. Ashraf, A. Sadhanala, P. Hayoz, J.-C. Flores, H. Sirringhaus, I. McCulloch, *Adv. Funct. Mater.* **2014**, *24*, 7109.
[17] R. S. Ashraf, A. J. Kronemeijer, D. James, H. Sirringhaus, I. McCulloch, *Chem. Commun.* **2012**, *48*, 3939 .
[18] H. J. Son, L. Lu, W. Chen, T. Xu, T. Zheng, B. Carsten, J. Strzalka, S. B. Darling, L. X. Chen, L. Yu, *Adv. Mater.* **2013**, *25*, 838.
[19] H. Kang, M. A. Uddin, C. Lee, K.-H. Kim, T. L. Nguyen, W. Lee, Y. Li, C. Wang, H. Y. Woo, B. J. Kim, *J. Am. Chem. Soc.* **2015**, *137*, 2359.
[20] H. K. H. Lee, Z. Li, I. Constantinou, F. So, S. W. Tsang, S. K. So, *Adv. Energy Mater.* **2014**, *4*, 1400768.
[21] J. Mei, K. R. Graham, R. Stalder, J. R. Reynolds, *Org. Lett.* **2010**, *12*, 660.
[22] G. Kim, A.-R. Han, H. R. Lee, J. Lee, J. H. Oh, C. Yang, *Chem. Commun.* **2014**, *50*, 2180.
[23] J. Kim, A.-R. Han, J. H. Seo, J. H. Oh, C. Yang, *Chem. Mater.* **2012**, *24*, 3464.
[24] W. Yue, T. He, M. Stolte, M. Gsänger, F. Würthner, *Chem. Commun.* **2014**, *50*, 545.
[25] L. Pandey, C. Risko, J. E. Norton, J.-L. Brédas, *Macromolecules* **2012**, *45*, 6405 .
[26] E. H. Jung, S. Bae, T. W. Yoo, W. H. Jo, *Polym. Chem.* **2014**, *5*, 6545.
[27] J. Kirkpatrick, C. B. Nielsen, W. Zhang, H. Bronstein, R. S. Ashraf, M. Heeney, I. McCulloch, *Adv. Energy Mater.* **2012** , *2* , 260 .
[28] Z. He, C. Zhong, S. Su, M. Xu, H. Wu, Y. Cao, *Nat. Photonics* **2012**, *6*, 591.
[29] R. S. Ashraf, I. Meager, M. Nikolka, M. Kirkus, M. Planells, B. C. Schroeder, S. Holliday, M. Hurhangee, C. B. Nielsen, H. Sirringhaus, I. McCulloch, *J. Am. Chem. Soc.* **2015**, *137*, 1314 .
[30] T.-Y. Chu, J. Lu, S. Beaupré, Y. Zhang, J.-R. Pouliot, J. Zhou, A. Najari, M. Leclerc, Y. Tao, *Adv. Funct. Mater.* **2012**, *22*, 2345.
[31] T. Lei, Y. Cao, Y. Fan, C.-J. Liu, S.-C. Yuan, J. Pei, *J. Am. Chem. Soc.* **2011**, *133*, 6099.
[32] F. C. Jamieson, E. B. Domingo, T. McCarthy-Ward, M. Heeney, N. Stingelin, J. R. Durrant, *Chem. Sci.* **2012**, *3*, 485.
[33] B. P. Lyons, N. Clarke, C. Groves, *Energy Environ. Sci.* **2012**, *5*, 7657.
[34] S. Shoaee, S. Subramaniyan, H. Xin, C. Keiderling, P. S. Tuladhar, F. Jamieson, S. A. Jenekhe, J. R. Durrant, *Adv. Funct. Mater.* **2013**, *23*, 3286.
[35] M. Scarongella, A. A. Paraecattil, E. Buchaca-Domingo, J. D. Douglas, S. Beaupre, T. McCarthy-Ward, M. Heeney, J.-E. Moser, M. Leclerc, J. M. J. Frechet, N. Stingelin, N. Banerji, *J. Mater. Chem. A.* **2014**, *2*, 6218.